CHAPTER 6

EFFECTS OF CHEMICAL REACTION, THERMAL RADIATION AND INTERNAL HEAT GENERATION ON CHEMICALLY REACTING MHD BOUNDARY LAYER FLOW OF HEAT AND MASS TRANSFER PAST A MOVING VERTICAL PLATE WITH SUCTION/INJECTION

6.1 INTRODUCTION

Boundary-layer flow over a moving plate is of great importance in view of their relevance to a wide variety of technical applications, particularly in the manufacture of fibers in glass and polymer industries. Flow through a porous medium have numerous engineering and geophysical applications, for example, in chemical engineering for filtration and purification process; in agriculture engineering to study the underground water resources; in petroleum technology to study the movement of natural gas, oil and water through the oil reservoirs. In view of these applications, many researchers have studied MHD free convective heat and mass transfer flow in a porous medium. In the boundary-layer theory, similarity solutions are found to be useful in the interpretation of certain fluid motions at large Reynolds numbers. Similarity solutions often exist in the flow over a semi-infinite plates and stagnation point flow for two dimensional, axi-symmetric and three dimensional bodies. In some special cases, when there is no similarity solution, one has to solve a system of nonlinear Partial Differential Equations (PDEs). The flow of an incompressible fluid past a moving surface has

several engineering applications. The aerodynamic extrusion of plastic sheets, the cooling of a large metallic plate in a cooling bath, the boundary layer along a liquid film in condensation process and a polymer sheet or filament extruded continuously from a die, or a long thread travelling between a feed roll and a wind-up roll are the examples of practical applications of a continuous flat surface. The free-convection flow with thermal radiation and mass transfer past a moving vertical porous plate was investigated by Makinde (2010). Olanrewaju et al (2012a) examined the effect of a transient free convective flow with radiative heat transfer past a flat plate moving through a binary mixture. In line with that, Mahdy (2010a) examined Soret and Dufour effect on double diffusion mixed convection from a vertical surface in a porous medium.

For similarity boundary-layer flows, velocity profiles are similar. But, this kind of similarity is lost for non-similarity flows Massoudi (2001). Obviously, the non-similarity boundary-layer flows are more general in nature and more important not only in theory but also in applications. Convective flow in porous media have been widely studied in the recent years due to its wide applications in engineering as post accidental heat removal in nuclear reactors, solar collectors, drying processes, heat exchangers, geothermal and oil recovery, building construction, etc. Nield & Bejan (2006), Ingham & Pop (2005), Vafai (2005), Vadasz (2008), have investigated the problems in the above area extensively. It is well known that conventional heat transfer fluids, including oil, water, and ethylene glycol mixture are poor heat transfer fluids, since the thermal conductivity of these fluids plays an important role on the heat transfer coefficient between the heat transfer medium and the heat transfer surface.

There has been considerable interest in studying the effect of chemical reaction and the heat source effect on the boundary layer flow problem with heat and mass transfer of an electrically conducting fluid in different geometry by Chakrabarti & Gupta (1979). Ibrahim et al (2008) studied the effect of chemical reaction and radiation absorption in the unsteady MHD free convection flow past a semi-infinite vertical permeable moving plate with a heat source and suction. Jat & Chaudhary (2010) studied the flow of incompressible viscous conducting fluid past a continuous moving surface in the presence of transverse magnetic field. Mahdy (2010b) has studied the effect of chemical reaction and heat generation or absorption on double diffusive convection from the vertical truncated cone in a porous media with variable viscosity.

In this chapter the numerical solution is presented in the study the effects of thermal radiation, chemical reaction, internal heat generation on chemically reacting MHD boundary layer flow of heat and mass transfer past a moving vertical plate with suction/injection.

6.2 ANALYSIS

Consider the steady free convective heat and mass transfer flow of a viscous, incompressible and electrically conducting fluid past a moving vertical plate with suction/injection. The non-uniform transverse magnetic field B_0 is imposed along the y-axis. The induced magnetic field is neglected as the magnetic Reynolds number of the flow is taken to be very small. It is also assumed that the external electric field is zero and the electric field due to polarization of charges is negligible. The temperature and the concentration of the ambient fluid are T_∞ and C_∞, and those at the surface are T_w (x) and C_w (x), respectively. It is also assumed that the pressure gradient, viscous and electrical dissipation are neglected. The fluid properties

are assumed to be constant except the density in the buoyancy terms of the linear momentum equation which is approximated according to the Boussinesq's approximation. Under the above assumptions, the boundary layer form of the governing equations can be written as

$$\frac{\partial u}{\partial x}+\frac{\partial v}{\partial y}=0 \tag{6.1}$$

$$u\frac{\partial u}{\partial x}+v\frac{\partial u}{\partial y}=\nu\frac{\partial^2 u}{\partial y^2}+g\beta_T\left(T-T_\infty\right)+g\beta_C\left(C-C_\infty\right)-\frac{\sigma {B_0}^2 u}{\rho} \tag{6.2}$$

$$u\frac{\partial T}{\partial x}+v\frac{\partial T}{\partial y}=\alpha\frac{\partial^2 T}{\partial y^2}+-\frac{\alpha_1}{\rho}\frac{\partial q_r}{\partial y}+Q\left(T-T_\infty\right) \tag{6.3}$$

$$u\frac{\partial C}{\partial x}+v\frac{\partial C}{\partial y}=D_m\frac{\partial^2 C}{\partial y^2}-R\left(C-C_\infty\right) \tag{6.4}$$

The boundary conditions for Equations (6.1)-(6.4) are expressed as

$$v=V,\quad u=Bx,\quad T=T_w=T_\infty+ax,\quad C=C_w=C_\infty+bx \quad \text{at } y=0$$

$$u\to 0,\ T\to T_\infty,\ C\to C_\infty \quad \text{as } y\to\infty \tag{6.5}$$

where B is a constant, a and b denotes the stratification rate of the gradient of ambient temperature and concentration profiles, (u, v) are the velocity components in x- and y- directions, respectively, T is the temperature, β_T is the volumetric coefficient of thermal expansion, α_1 is the thermal diffusivity, g is the acceleration due to gravity, υ is the kinematic viscosity, D_m is the coefficient of diffusion in the mixture, C is the species concentration, σ is the electrical conductivity, B_o is the externally imposed magnetic field in the y-direction.

Using the Roseland approximation, the radiative heat flux in the y-direction is given by

$$q_r = -\frac{4\sigma^*}{3K'}\frac{\partial T^4}{\partial y} \tag{6.6}$$

where σ^* and K' are the Stefan – Boltzmann constant and the mean absorption coefficient, respectively. We assume that the temperature differences within the flow are sufficiently small so that the T^4 can be expressed as a linear function after using Taylor series to expand T^4 about the free stream temperature T_∞ and neglecting higher order terms. This result is

$$T^4 \approx 4T_\infty^3 T - 3T_\infty^4 \tag{6.7}$$

Using the Equations (6.6) and (6.7) in the Equation (6.3), we obtain

$$\frac{\partial q_r}{\partial y} = -\frac{16\sigma^*}{3K}\frac{\partial T^4}{\partial y} \tag{6.8}$$

We non-dimensionalize the Equations (6.1) to (6.4) using the following transformations:

$$\eta = \sqrt{\frac{B}{\nu}}y, \qquad f(\eta) = \frac{\psi}{x\sqrt{B\nu}}, \quad \theta(\eta) = \frac{T - T_\infty}{T_w - T_\infty}, \quad \phi(\eta) = \frac{C - C_\infty}{C_w - C_\infty} \tag{6.9}$$

where ψ is the stream function defined by $u = \frac{\partial \psi}{\partial x}$ and $v = -\frac{\partial \psi}{\partial y}$ in order to satisfy the continuity Equation (6.1). In the equations $f(\eta)$ is a dimensionless stream function, $\theta(\eta)$ is a dimensionless temperature of the fluid in the boundary layer region, $\phi(\eta)$ is a dimensionless species concentration of the

fluid in the boundary layer region and η is the similarity variable. The velocity components u and v are respectively obtained as follows

$$u = \frac{\partial \psi}{\partial y} = xBf' \qquad v = -\frac{\partial \psi}{\partial x} = -\sqrt{B\nu}\, f \tag{6.10}$$

where $F_w = \dfrac{V}{\sqrt{B\nu}}$ is the dimensionless suction velocity.

The partial differential Equations (6.2) - (6.4) are transformed into local similarity equations as follows using the Equations (6.9) and (6.10).

$$f''' + f f'' - (f' + M) f' + G_r \theta + G_c \phi = 0 \tag{6.11}$$

$$\theta'' \left(1 + \frac{4}{3} R\right) + \Pr\left(f \theta' - f' \theta\right) + \Pr \alpha \theta = 0 \tag{6.12}$$

$$\varphi'' + Sc\left(f \varphi' - f' \varphi\right) - Sc\gamma\varphi = 0 \tag{6.13}$$

where primes denote differentiation with respect to η. The appropriate flat free convection boundary conditions are also transform into the form,

$$\begin{aligned} &f' = 1,\ f = -F_w,\ \theta = 1,\ \varphi = 1 \quad at\ \ \eta = 0 \\ &f' = 0,\ \theta = 0,\ \varphi = 0 \qquad\qquad as\ \eta \to \infty \end{aligned} \tag{6.14}$$

where $M = \dfrac{\sigma B_0^2}{\rho B}$ is the magnetic parameter

$\Pr = \dfrac{\nu}{\alpha}$ is the Prandtl number

$Sc = \frac{\nu}{D_m}$ is the Schmidt number

$G_r = \frac{g\beta_T (T_w - T_\infty)}{xB^2}$ is the local temperature Grashof number

$G_c = \frac{g\beta_c (C_w - C\infty)}{xB^2}$ is the local concentration Grashof number

$\alpha = \frac{Q}{B\alpha_1}$ is the internal heat generation

$\gamma = \frac{\nu R}{B^2}$ is the chemical reaction parameter

The quantities of physical interest in this problem are local skin friction, the local Nusselt number and the local Sherwood number.

6.3 COMPUTATIONAL PROCEDURE

The set of Equations (6.11) to (6.13) together with the boundary conditions as given in the Equation (6.14) have been solved numerically by applying Runge-Kutta Gill method with shooting technique. From the process of numerical computation, the skin-friction coefficient, the local Nusselt number and the local Sherwood number, which are respectively proportional to f "(0) , -θ ' (0) *and*- ϕ'(0) , are also sorted out and their numerical values are presented in a tabular form. The computations have been performed by a program which uses Fortran 7.7. A step size of $\Delta\eta = 0.001$ is selected to be satisfactory for a convergence criterion of 10^{-7} in nearly all cases. The value of *y* is found to each iteration loop by the assignment statement $\eta_\infty = \eta_\infty + \Delta\eta$. The maximum value of η_∞ , to each group of parameters, *Pr*, *Sc*, *M*, *R*, G_T,

G_C, K , S, α and γ is determined when the values of unknown boundary conditions at $\eta = 0$ do not change to successful loop with error less than 10^{-7}.

6.4 RESULTS AND DISCUSSION

In order to get a clear insight of the physical problem, the velocity, temperature and concentration have been discussed by assigning numerical values to the parameters encountered in the problem. To be realistic, the values of the embedded parameters were chosen following Ibrahim et al (2008). Attention is focused on positive values of the buoyancy parameters, i.e. Grashof number $G_T > 0$ (which corresponds to the cooling problem) and solutal Grashof number $G_C > 0$ (which indicates that the chemical species concentration in the free stream region is less than the concentration at the boundary surface) and the volumetric heat generation/absorption parameter. The cooling problem is often encountered in engineering applications. In Table 6.1 it generates the skin friction coefficient, Nusselt number and the Sherwood number for any embedded parameter value in the flow model.

It is clearly seen that an increase in the parameters M, Sc, Pr, Ra, and γ leads to an increase in the skin-friction at the wall plate while the increase in parameters Gr, Gc, f_w and α decreases the skin-friction at the wall surface. Similarly, the Nusselt number increases at the wall plate when Gr, G_C, f_w, Pr and Ra increases while it decreases at the wall plate when parameters M, α and γ increases. It is interesting to note that the Sherwood number on the wall plate increases with increase in Gc, M, Sc, Pr, α and γ decreases with other parameters embedded in the flow model.

Table 6.1 Values of f''(0), -θ'(0) and -ϕ'(0) for various values of embedded flow parameters

Gr	*Gc*	*M*	*Fw*	*Sc*	*Pr*	α	γ	Ra	f '' (0)	-θ'(0)	-ϕ'(0)
0.1	0.1	0.1	0.1	0.62	0.72	1	1	0.1	0.6857050	2.521404	1.202090
0.5	0.1	0.1	0.1	0.62	0.72	1	1	0.1	0.4766934	0.165968	1.172184
1.0	0.1	0.1	0.1	0.62	0.72	1	1	0.1	0.2377260	0.1739780	1.183749
0.1	0.5	0.1	0.1	0.62	0.72	1	1	0.1	0.5501700	2.331515	1.205999
0.1	1.0	0.1	0.1	0.62	0.72	1	1	0.1	0.3819476	2.102049	1.210881
0.1	0.1	1.0	0.1	0.62	0.72	1	1	0.1	0.9925398	5.877328	1.251050
0.1	0.1	1.5	0.1	0.62	0.72	1	1	0.1	1.1493539	7.687298	1.279015
0.1	0.1	0.1	1.0	0.62	0.72	1	1	0.1	0.4673465	1.810943	0.898195
0.1	0.1	0.1	2.0	0.62	0.72	1	1	0.1	0.3516448	0.705366	0.662772
0.1	0.1	0.1	-0.1	0.62	0.72	1	1	0.1	0.7321387	2.927027	1.286751
0.1	0.1	0.1	-1.0	0.62	0.72	1	1	0.1	1.2234841	2.573560	1.618071
0.1	0.1	0.1	0.1	0.78	0.72	1	1	0.1	0.6662407	2.810866	1.358596
0.1	0.1	0.1	0.1	2.62	0.72	1	1	0.1	0.6773186	2.854431	2.457772
0.1	0.1	0.1	0.1	0.62	1.0	1	1	0.1	0.6754098	3.056807	1.223527
0.1	0.1	0.1	0.1	0.62	3.0	1	1	0.1	0.7792231	2.695652	1.230853
0.1	0.1	0.1	0.1	0.62	7.0	1	1	0.1	0.8675786	1.037836	1.169757
0.1	0.1	0.1	0.1	0.62	0.72	1	1	0.1	0.6742893	2.765831	1.389394
0.1	0.1	0.1	0.1	0.62	0.72	1	1	0.1	0.7156069	2.783903	2.392893
0.1	0.1	0.1	0.1	0.62	0.72	1	1	0.1	0.6648644	2.841222	1.212446
0.1	0.1	0.1	0.1	0.62	0.72	1	1	0.1	0.6641262	2.872122	1.213809
0.1	0.1	0.1	0.1	0.62	0.72	2	1	0.1	0.0934791	18.42139	1.669504
0.1	0.1	0.1	0.1	0.62	0.72	2.2	1	0.1	0.052747	23.56778	1.816335
0.1	0.1	0.1	0.1	0.62	0.72	1	2	0.1	0.668837	2.784687	1.439166

6.4.1 Velocity Profiles

The effects of various thermo physical parameters of the fluid velocity are illustrated in Figures 6.1 to 6.5. Figure 6.1 depicts the effect of magnetic strength parameter M on the fluid velocity and it can be observed a decrease in the fluid velocity as parameter *M* increases. This is because an increase in the magnetic strength parameter M stabilizes the fluid motion or flow. Figure 6.2 depicts the influence of the suction parameter F_w which decreases the fluid velocity while injection increases the fluid velocity. It is interesting to note that increasing thermal and solutal Grashof numbers (Gr, G_C) increase the fluid velocity as evident from Figures 6.3 and 6.4. In Figure 6.5, we display the graph of velocity profiles with various values of energy generation parameter α against span wise coordinate η. It is interesting to note that increasing the parameter α bring an increase in the fluid velocity.

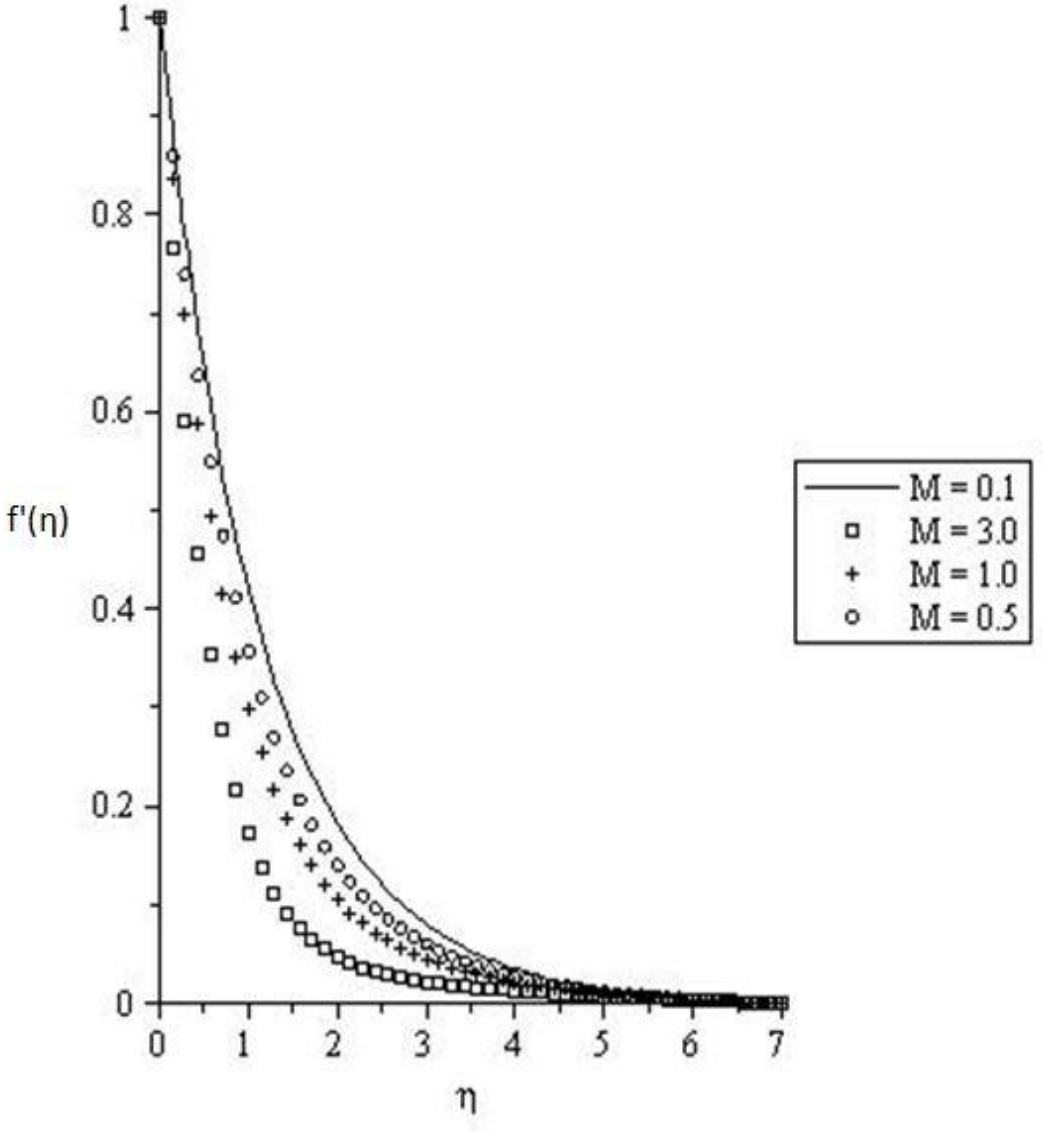

Figure 6.1 Velocity profiles for Gr = Gc = F_w = γ = α_i = R = 0.1, Pr = 0.72, Sc=0.62

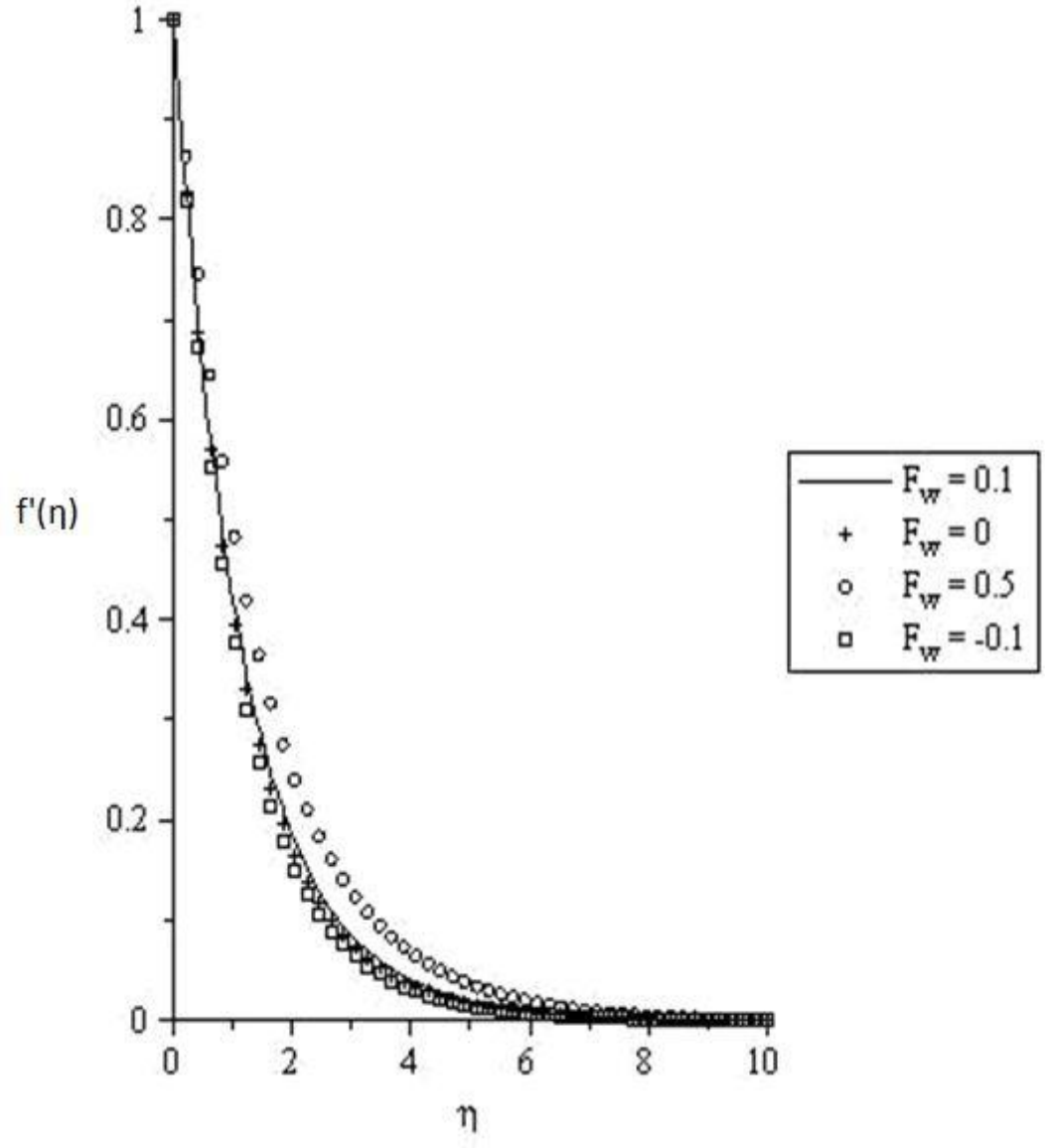

Figure 6.2 Velocity profiles for Gr = Gc = γ = α_i = R = M = 0.1, Pr = 0.7, Sc=0.62

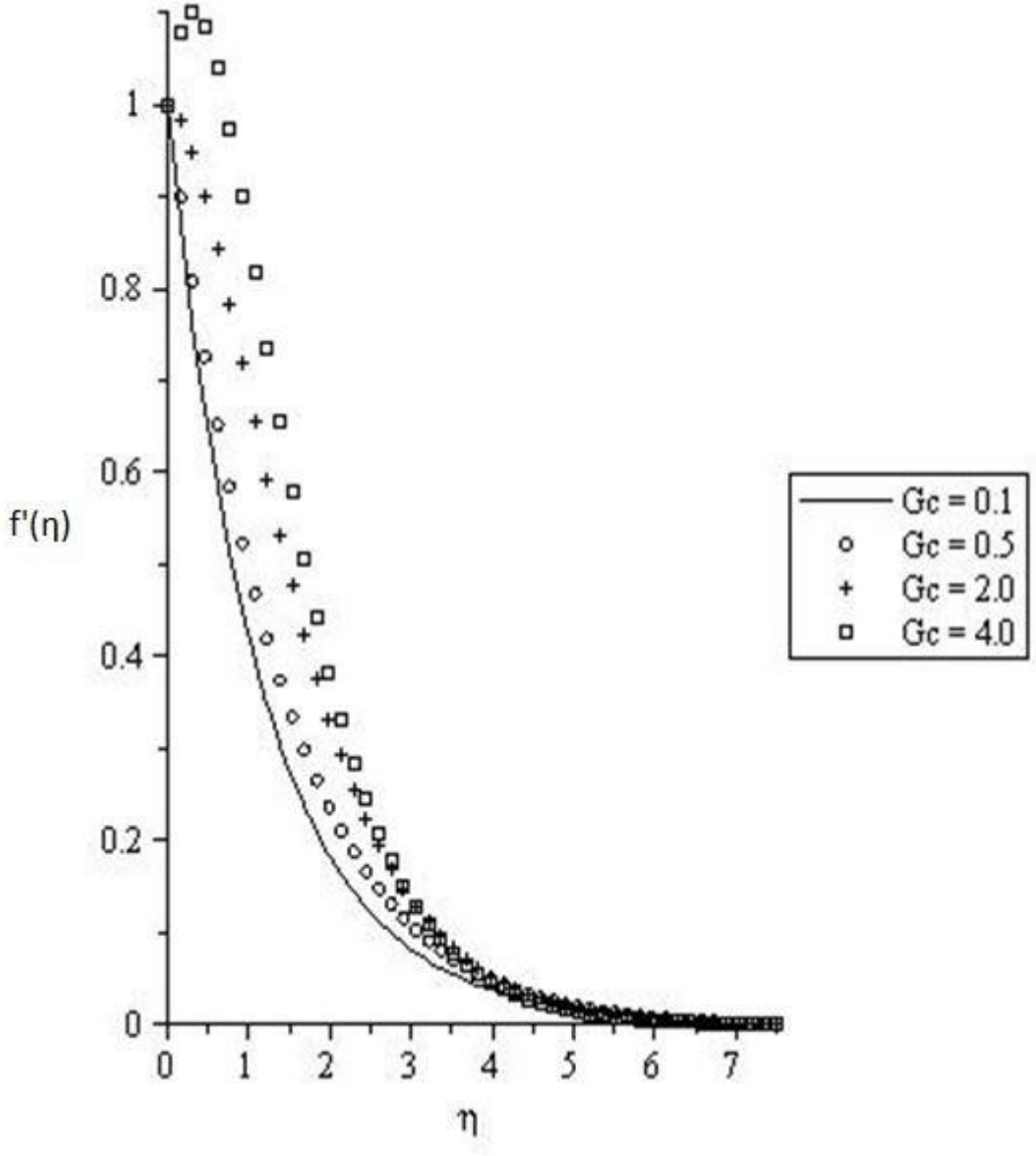

Figure 6.3 Velocity profiles for Gr = F_w = γ = α_i = R = M = 0.1, Pr = 0.72, Sc = 0.62

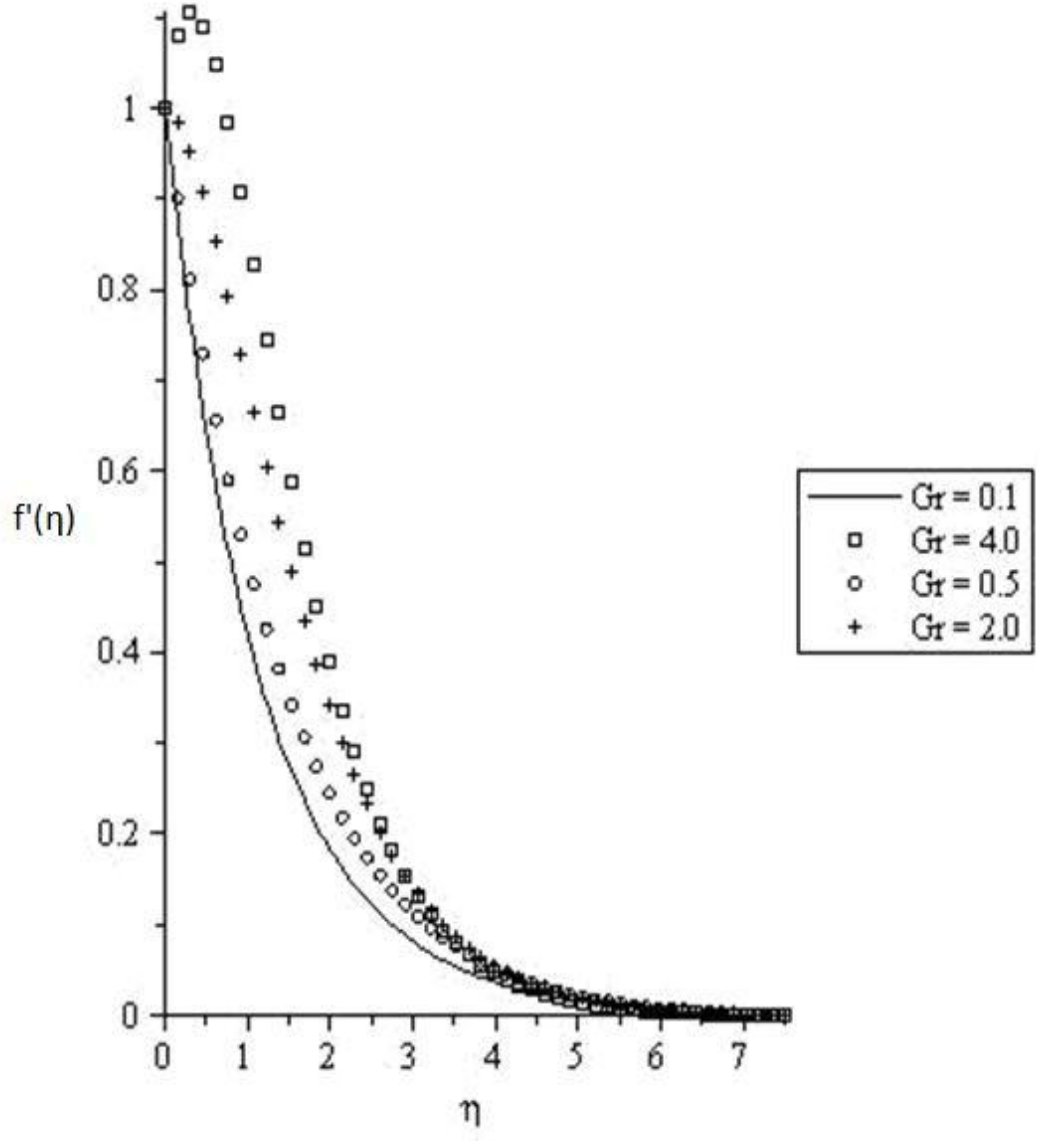

Figure 6.4 Velocity profiles for Gc = F_w = γ = α_i = R = M = 0.1, Pr = 0.72, Sc = 0.62

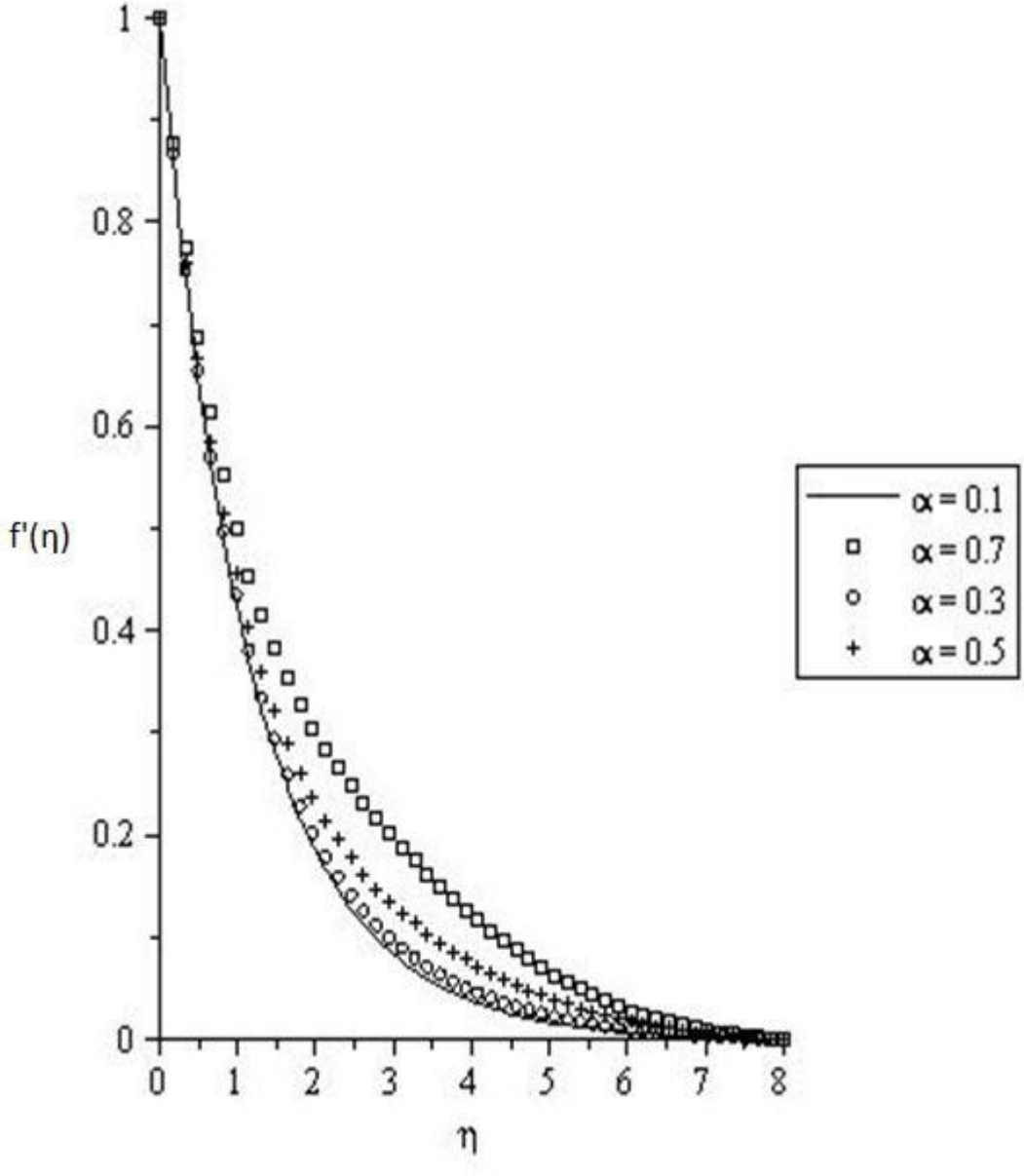

Figure 6.5 Velocity profiles for Gc = Gr = F_w = γ = R = M = 0.1, Sc = 0.62, Pr = 0.72.

6.4.2 Temperature Profiles

The influences of various embedded parameters on the fluid temperature are illustrated in Figures 6.6 to 6.12. Figure 6.6 depicts the graph of temperature against η for various values of magnetic strength parameter M. It is interesting to note that the thermal boundary layer thickness increases as M increases. In Figure 6.7, it is seen that suction decreases the thermal boundary layer thickness, while injection decreases the thermal boundary layer thickness. It is interesting to note that the thermal boundary layer thickness increases as the thermal and the solutal Grashof numbers increases as shown in Figures 6.8 and 6.9.

Figure 6.10 depicts the curve of temperature against span wise coordinate η for various values of Prandtl number *Pr*. It is clearly seen that increases in the Prandtl number decreases the temperature profile and thereby decreases the thermal boundary layer thickness. Fluids with high Prandtl number has low velocity, which in turn also implies that at lower fluid velocity the species diffusion is comparatively lower and hence higher species concentration is observed at high Prandtl number. Increase in the value of the internal heat generation parameter α and radiation parameter Ra increases the thermal boundary layer thickness as depicted in Figures 6.11 and 6.12.

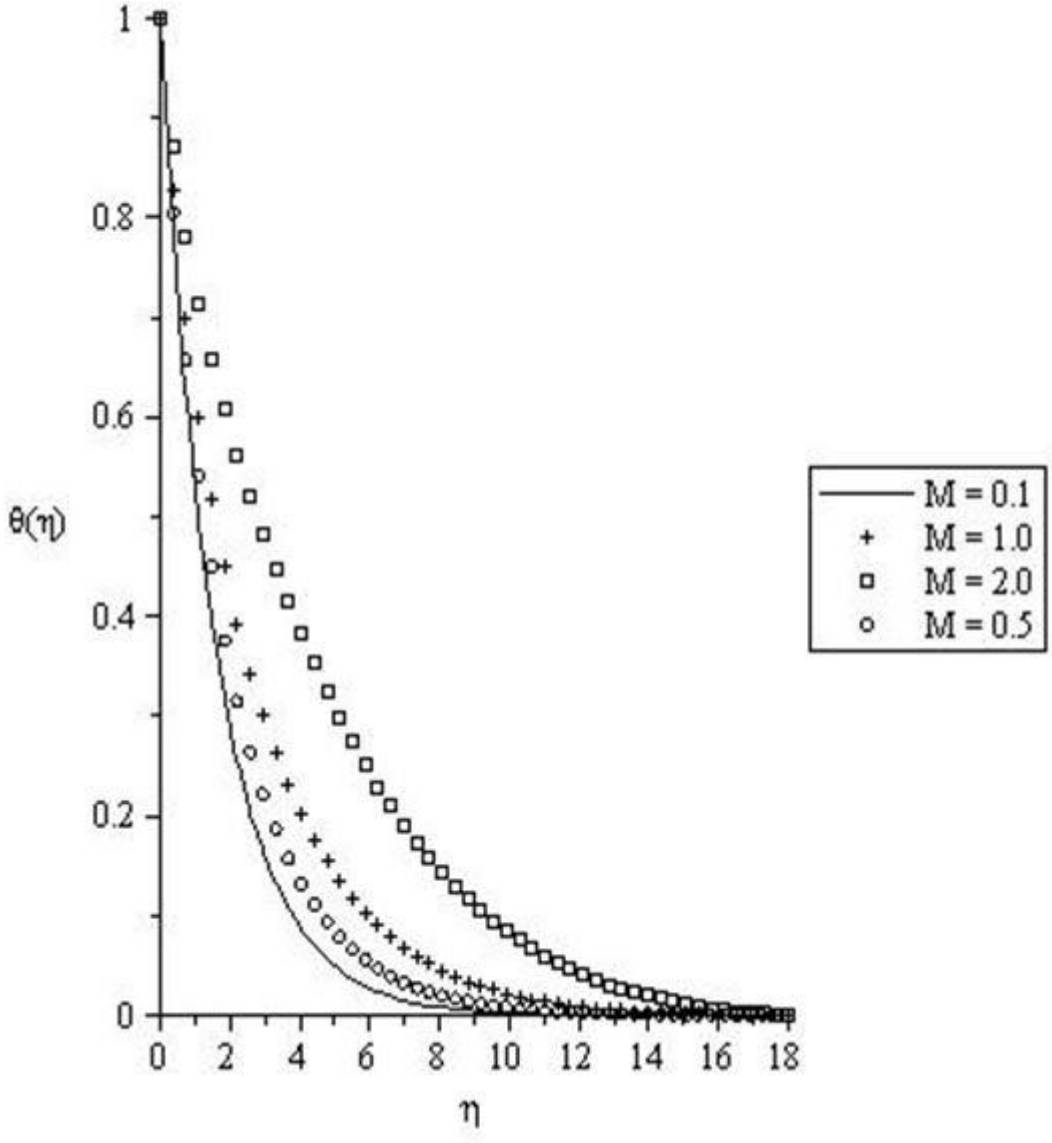

Figure 6.6 Temperature profiles for Gr = Gc = F_w = γ = α_i = R = 0.1, Pr = 0.72, Sc = 0.62

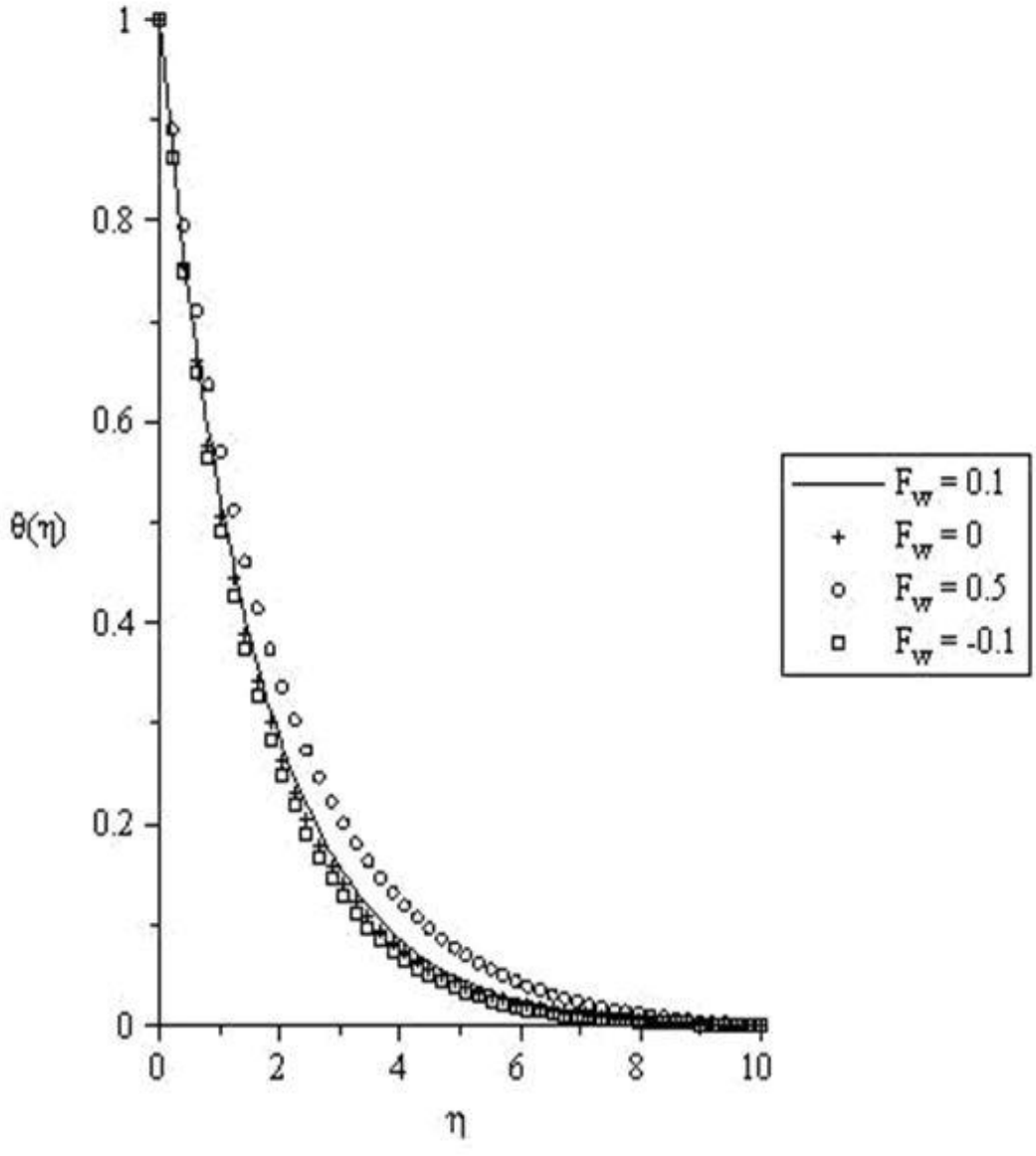

Figure 6.7 Temperature profiles for Gr = Gc = γ = α_i =0.1 and R = M = 0.1, Pr = 0.72, Sc = 0.62

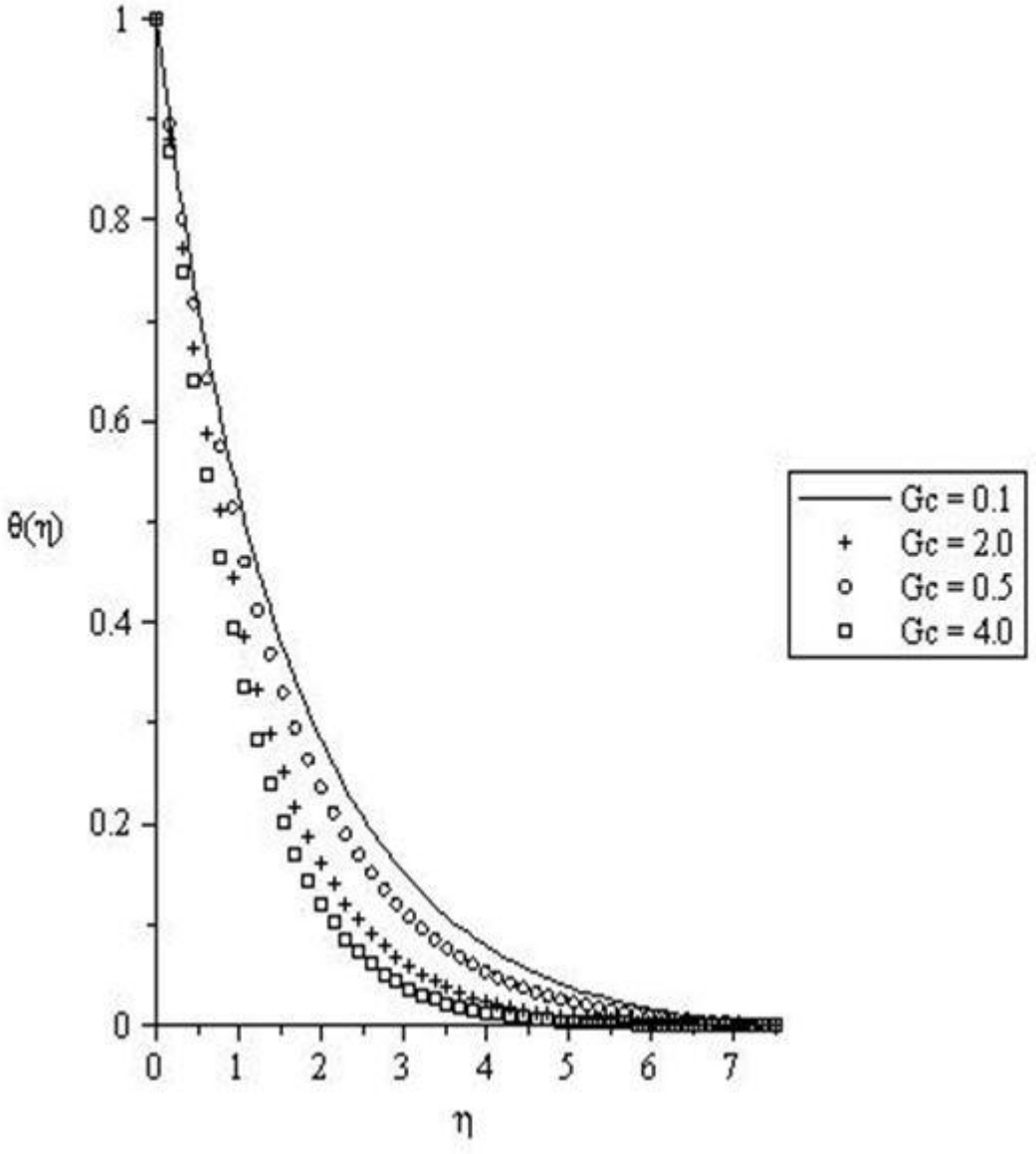

Figure 6.8 Temperature profiles for Gr = F_w = γ = α_i = 0.1 and R = M = 0.1, Pr = 0.72, Sc = 0.62

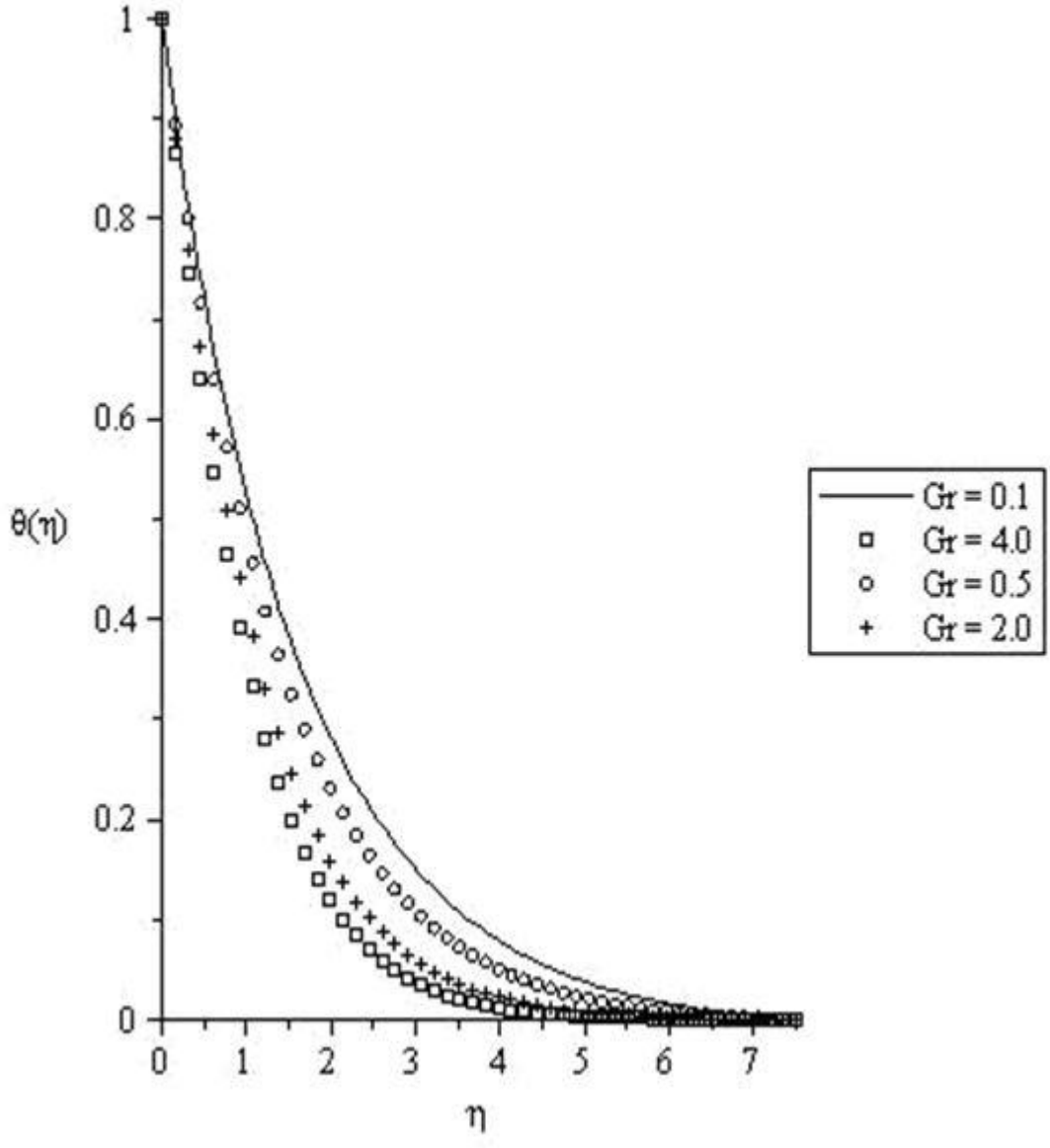

Figure 6.9 Temperature profiles for Gc = F_w = γ = α_i = 0.1 and R = M = 0.1, Pr = 0.72, Sc = 0.62

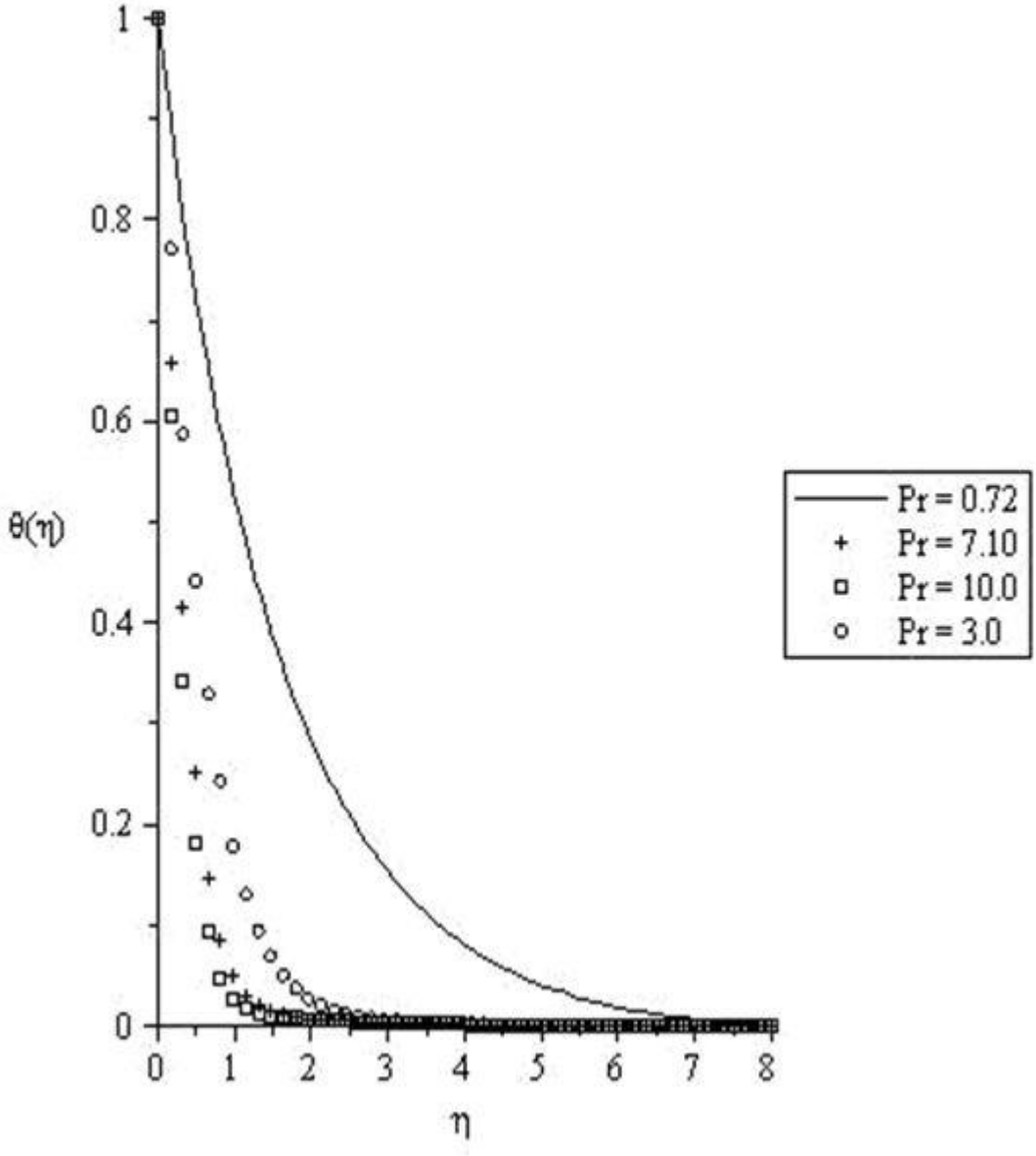

Figure 6.10 Temperature profiles for Gc = Gr = F_w = γ = α_i = 0.1 and Ra = M = 0.1, Sc = 0.62

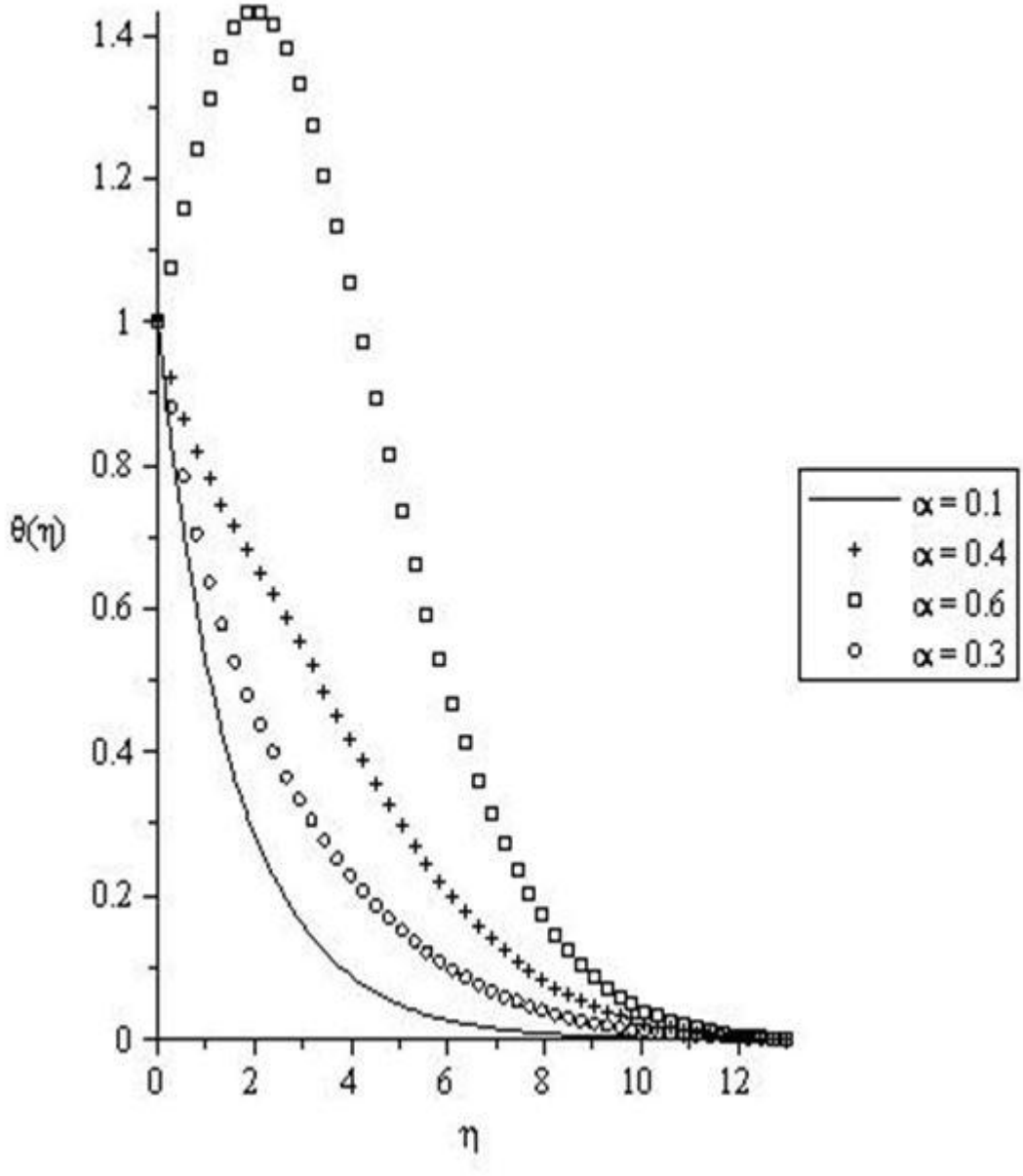

Figure 6.11 Temperature profiles for Gc = Gr = F_w = γ = 0.1 and R = M = 0.1, Sc = 0.62, Pr = 0.72

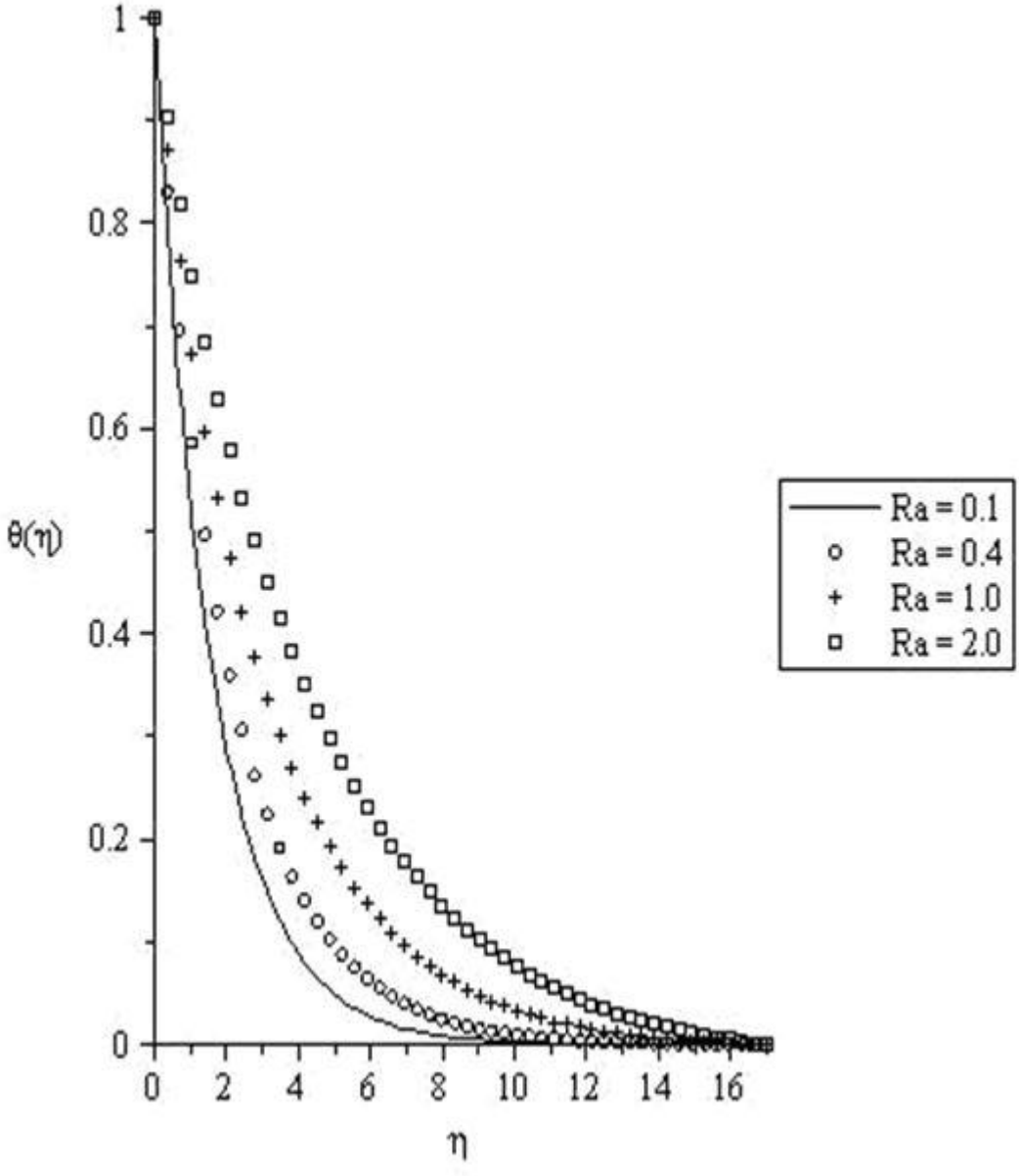

Figure 6.12 Temperature profiles for Gc = Gr = F_w = α_i = 0.1 and γ = M = 0.1, Sc = 0.62, Pr = 0.72

6.4.3 Concentration Profiles

The effects of various thermo physical parameters on the fluid concentration are illustrated in Figures 6.13 to 6.19. Figure 6.13 reflects that with increase in magnetic strength parameter M increases the fluid concentration. It is clearly seen that suction and injection has similar effects with velocity and temperature profiles. In Figures 6.15 and 6.16 it is clearly seen that the Grashof number decreases the concentration boundary layer thickness. Figure 6.17 depicts the curve of the concentration profile against η for various values of Schmidt number Sc. We notice that Sc is to decrease the concentration boundary layer thickness across the boundary. Internal heat generation and the chemical reaction parameters are to decrease the concentration boundary layer thickness as illustrated in figures 6.18 and 6.19. Figure 6.19 shows that if $\gamma > 0$ (destructive), the concentration decreases but if $\gamma < 0$ (generative), the concentration increases confirming the existing literatures.

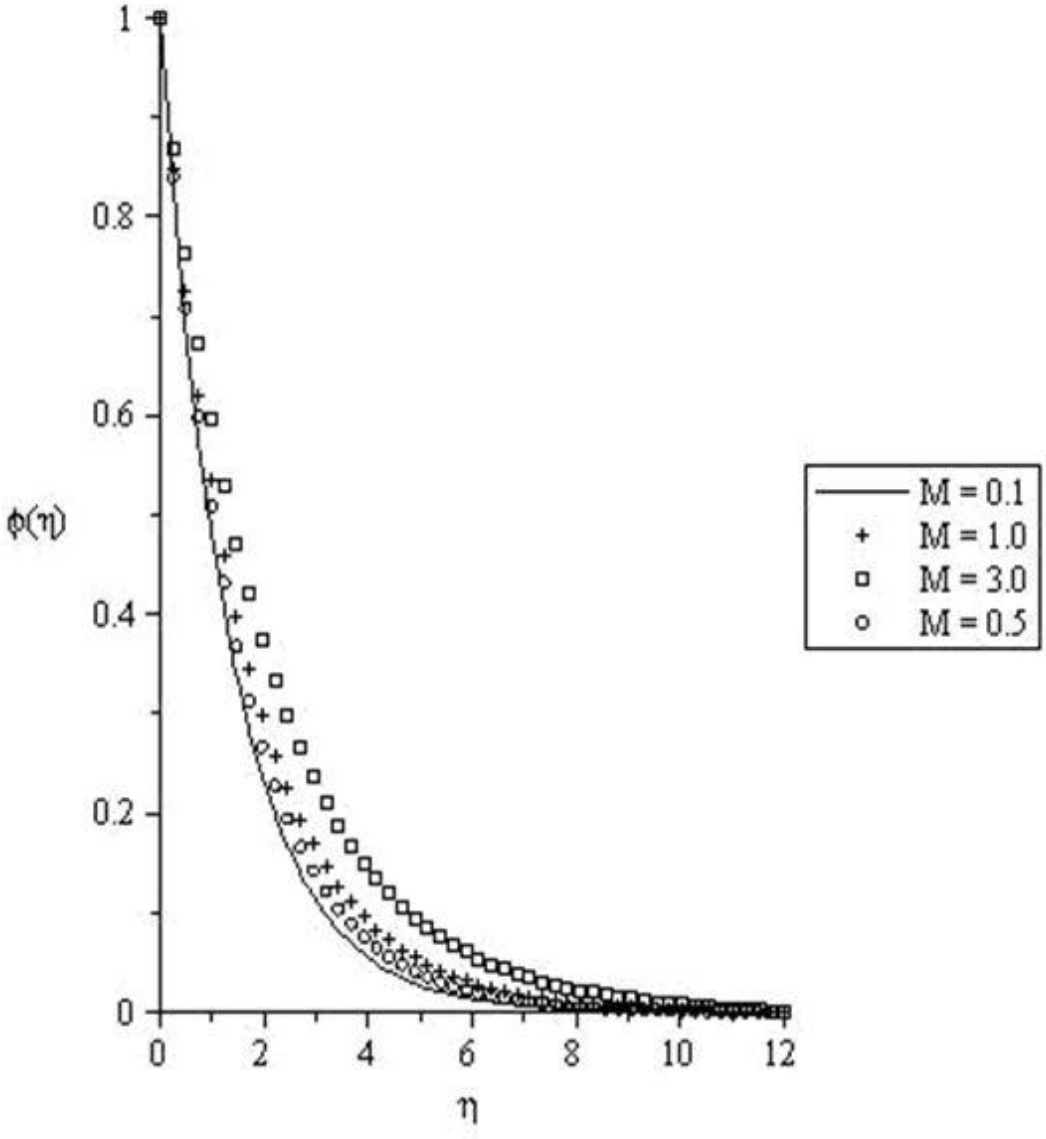

Figure 6.13 Concentration profiles for Gr = Gc = F_w = γ = α_i = 0.1 and Ra = 0.1, Pr = 0.72, Sc = 0.62

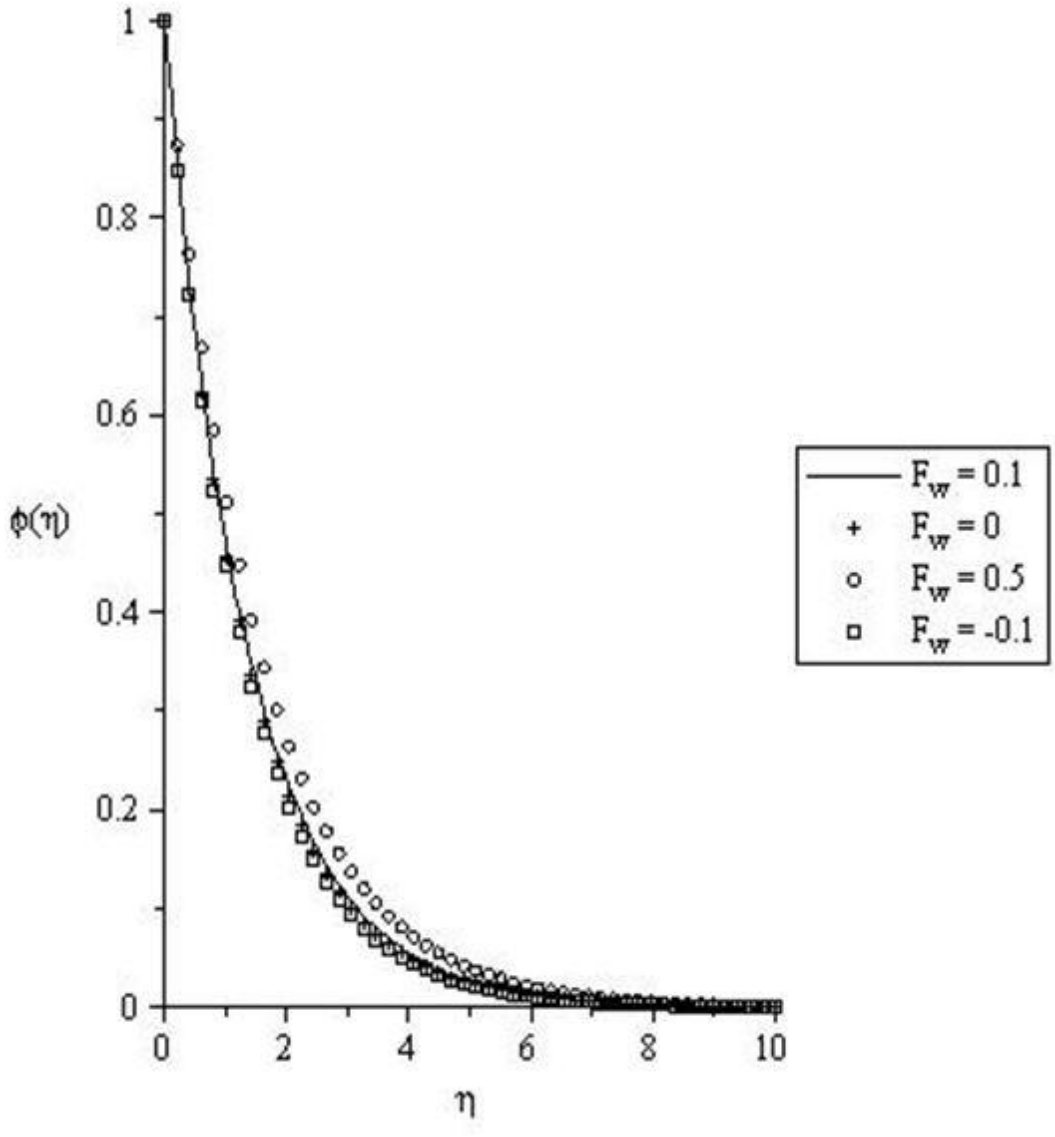

Figure 6.14 Concentration profiles for Gr = Gc = γ = α_i = 0.1 and Ra = M = 0.1, Pr = 0.72, Sc = 0.62

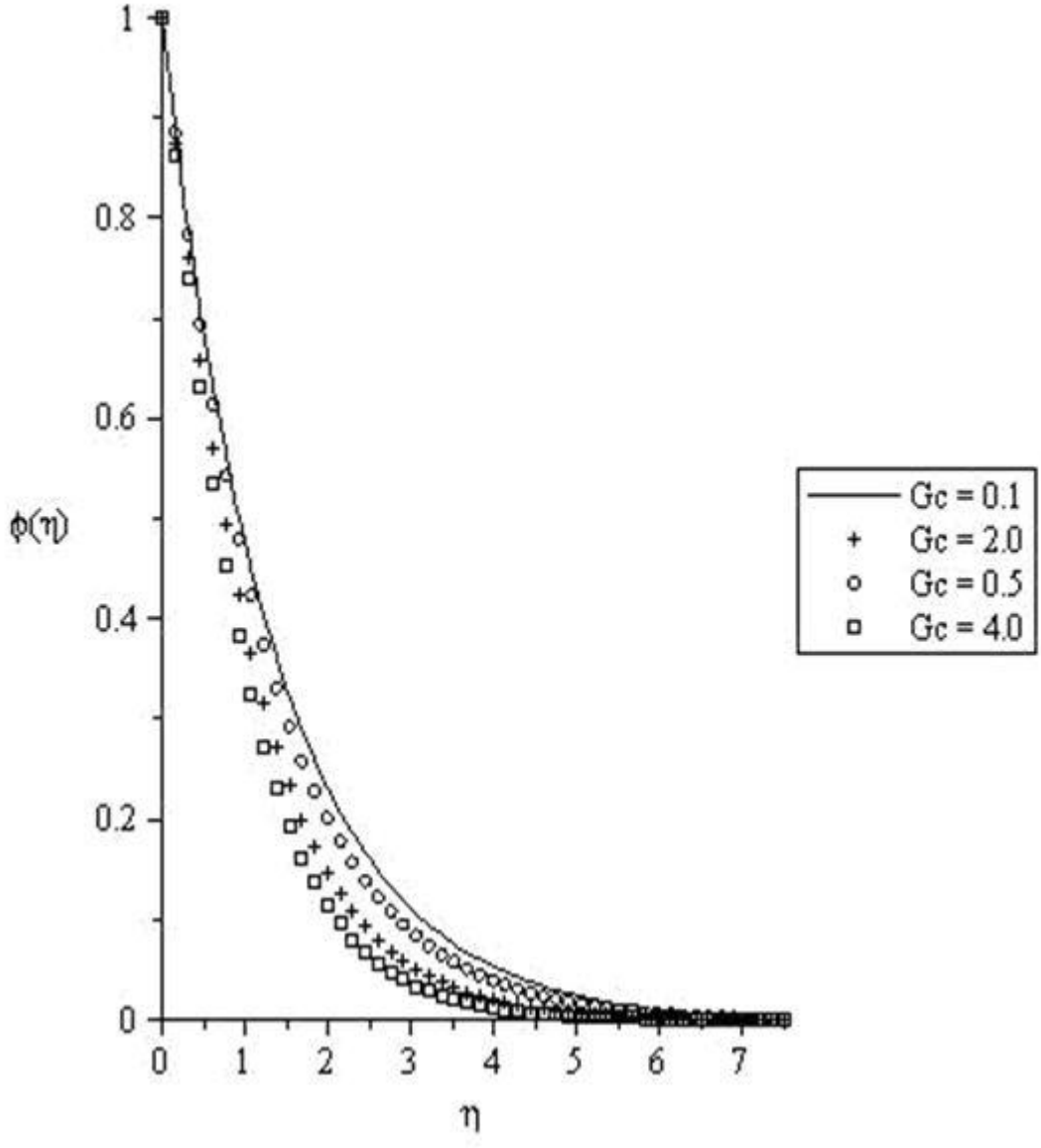

Figure 6.15 Concentration profiles for Gr = F_w = γ = α_i = 0.1 and Ra = M = 0.1, Pr = 0.72, Sc = 0.62

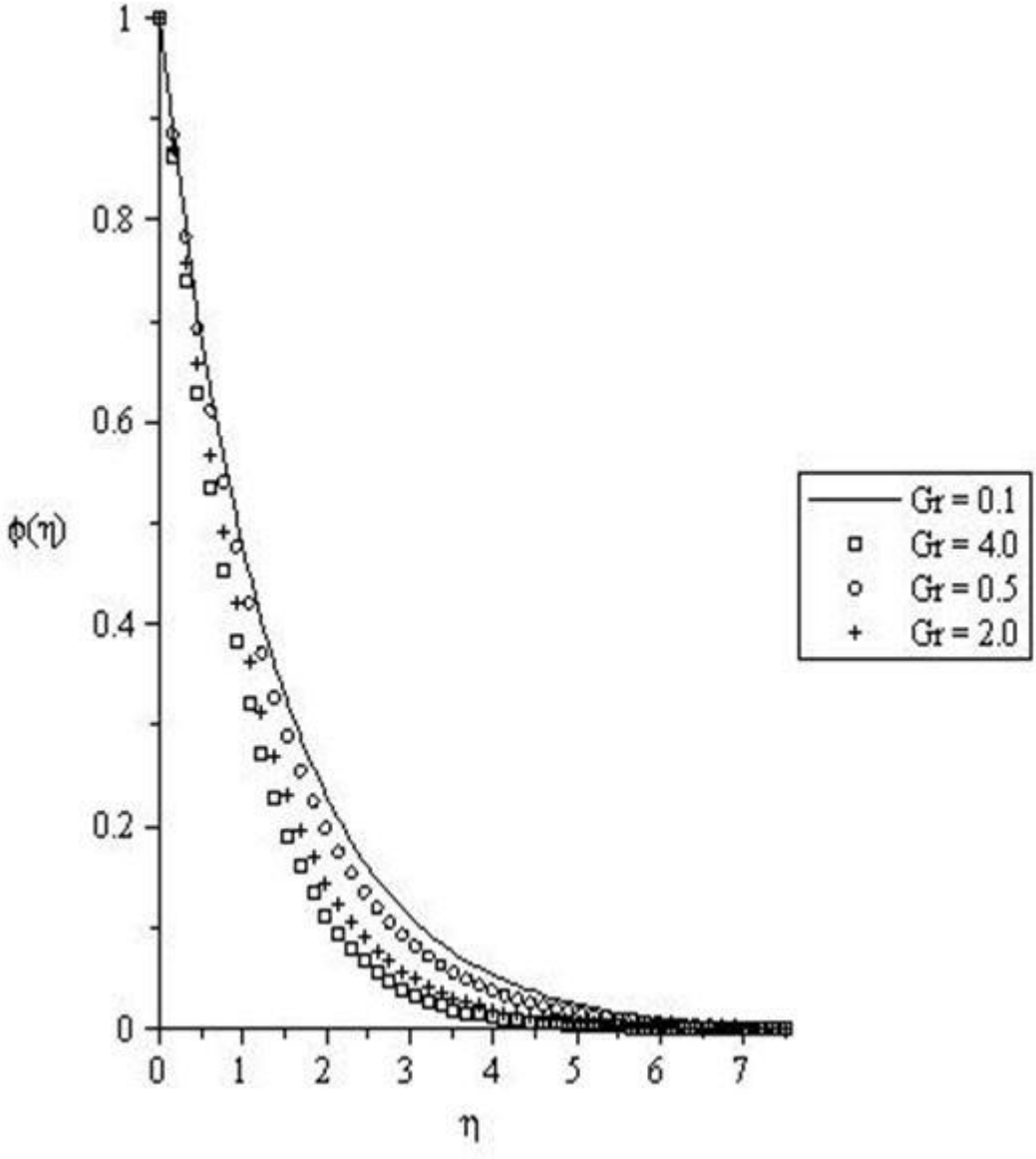

Figure 6.16 Concentration profiles for Gc = F_w = γ = α_i = 0.1 and Ra = M = 0.1, Pr = 0.72, Sc = 0.62

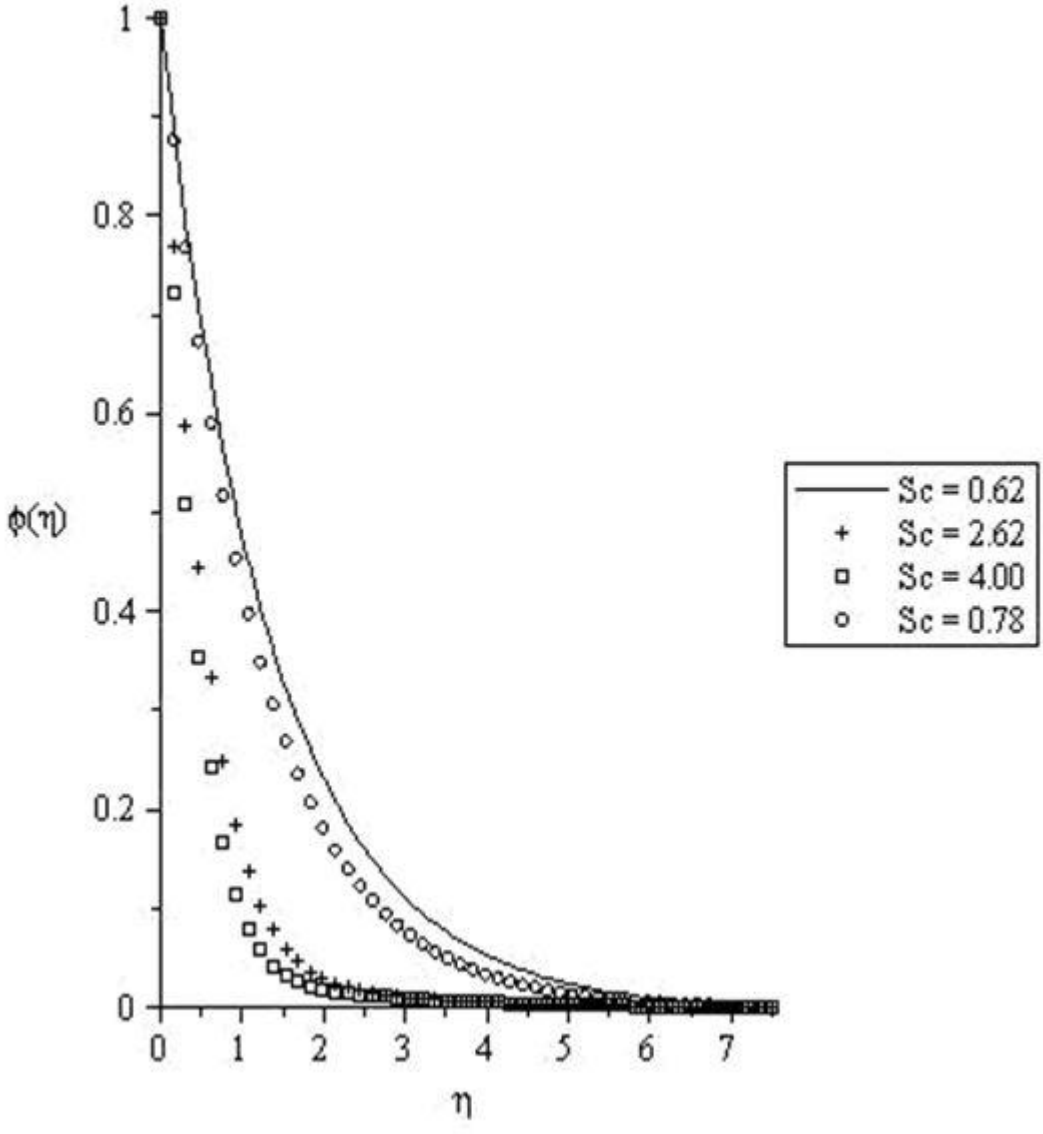

Figure 6.17 Concentration profiles for Gc = Gr = F_w = γ= α_i = 0.1 and Ra = M = 0.1, Pr = 0.72

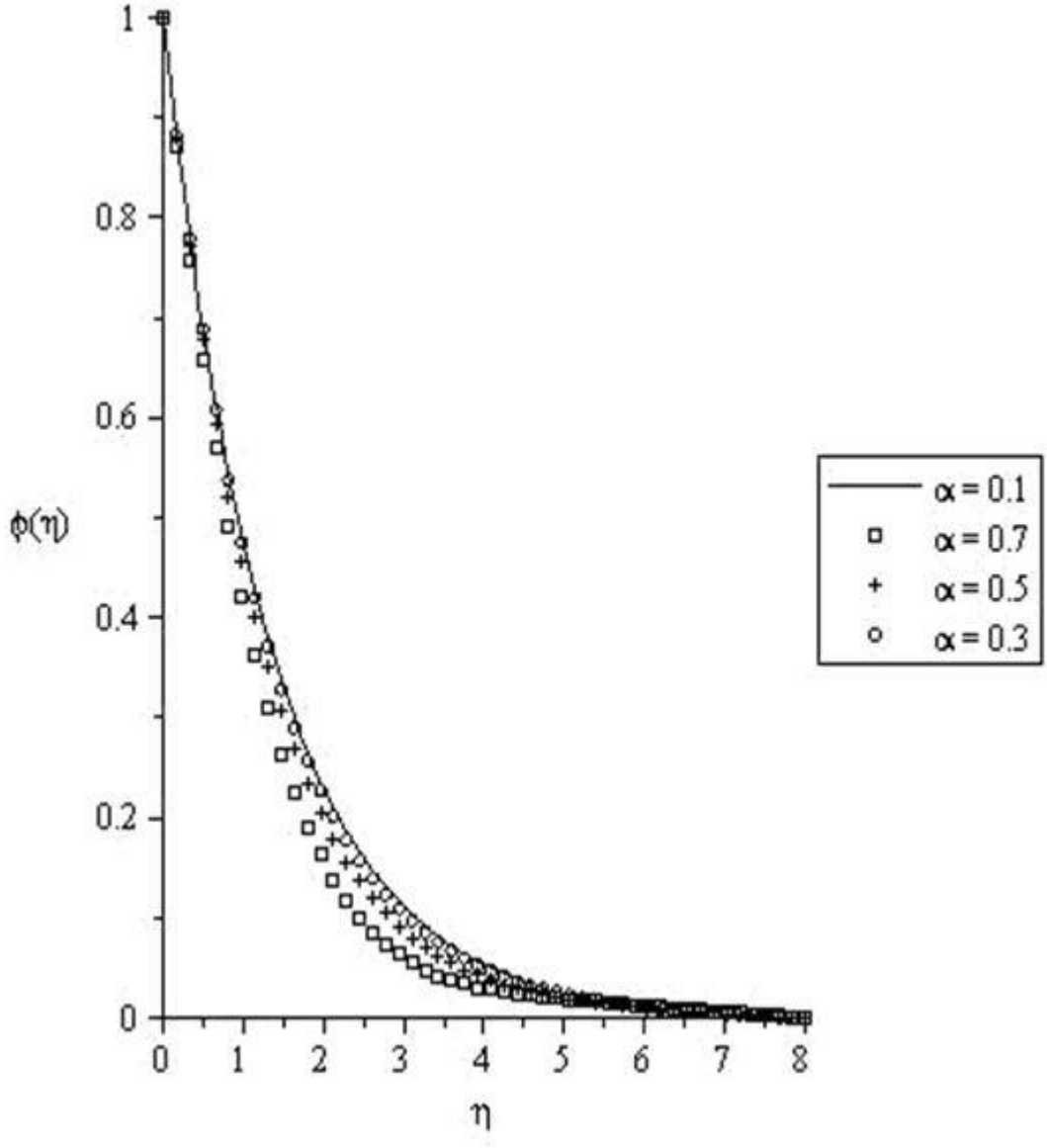

Figure 6.18 Concentration profiles for Gc = Gr = F_w = γ = 0.1 and Ra = M = 0.1, Sc = 0.62, Pr =0.72

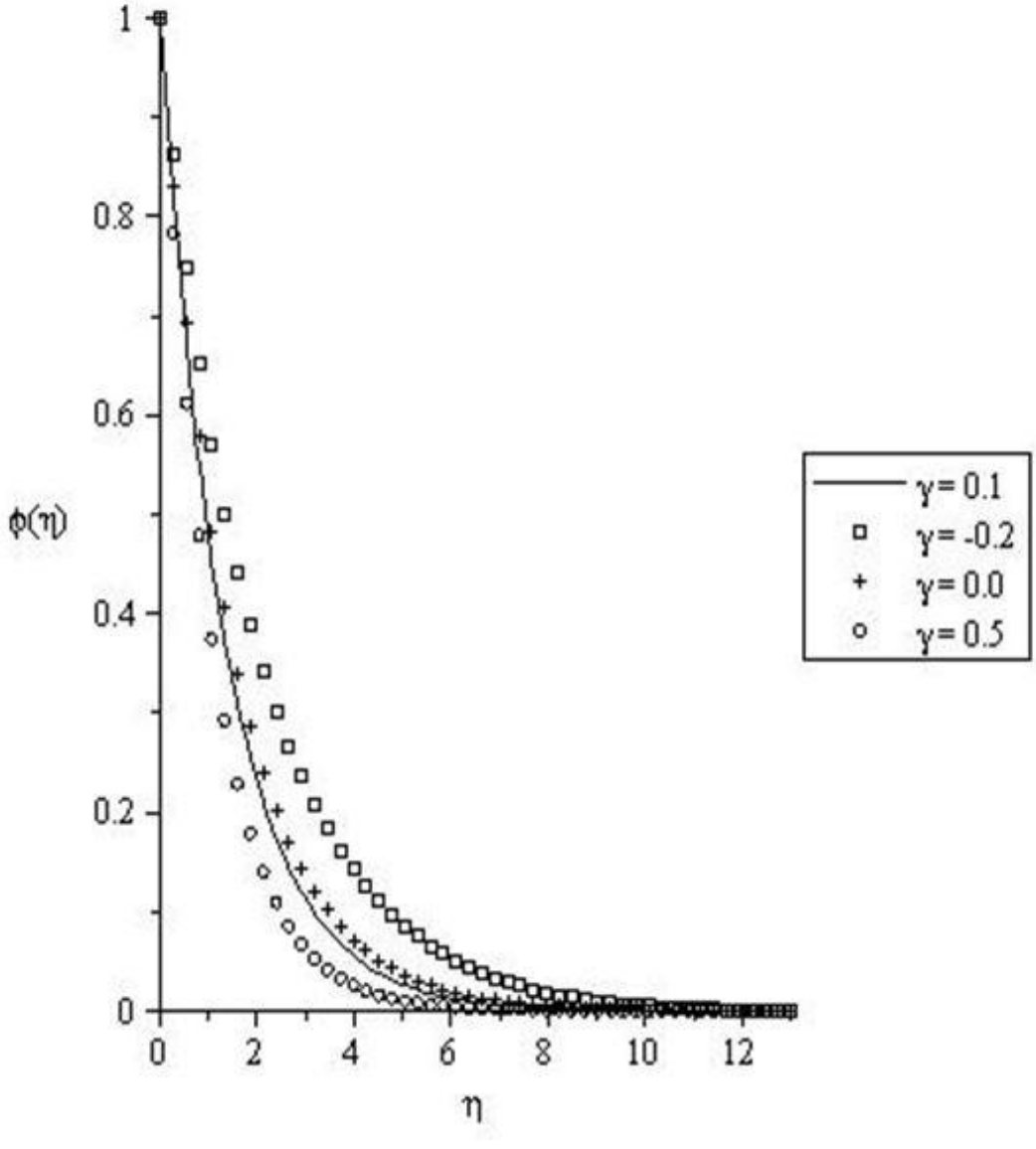

Figure 6.19 Concentration profiles for Gc = Gr = F_w = α_i = 0.1 and Ra = M = 0.1, Sc = 0.62, Pr = 0.72

6.5 CONCLUSION

The two-dimensional, steady, incompressible electrically conducting, laminar free convection boundary layer flow of a continuously moving vertical porous plate in a chemically reactive medium in the presence of transverse magnetic field, thermal radiation, chemical reaction, internal heat generation and with suction/injection have been investigated theoretically. The governing nonlinear partial differential equations have been reduced to the coupled nonlinear ordinary differential equations by the similarity transformations. The problem is solved numerically using shooting techniques with the Runge-Kutta Gill method. Comparison between the existing literature and the present study were carried out and found to be in excellent agreement. We extended the work of Ibrahim et al (2008) to include the magnetic field strength, the thermal radiation, internal heat generation and chemical reaction term to extend the physical application of the subject. Our results reveal among others, that the fluid velocity within the boundary layer decreases with increasing the magnetic strength and wall suction, and increases with wall injection. It was established that an increase in the wall suction enhances the boundary layer thickness and reduces the skin friction together with the heat and mass transfer rate at the moving plate surface. In addition, the chemical species concentration within the boundary layer decreases with increasing Gc, Gr, Sc and α.